The Journal of Experimental Biology 201, 2091–2102 (1998)
Printed in Great Britain © The Company of Biologists Limited 1998
JEB1583

REVIEW

THE ELECTRONEUTRAL CATION–CHLORIDE COTRANSPORTERS

DAVID B. MOUNT[1], ERIC DELPIRE[2], GERARDO GAMBA[3], AMY E. HALL[1], ESTEBAN POCH[4], ROBERT S. HOOVER JR[1] AND STEVEN C. HEBERT[1,*]

[1]*Department of Medicine and* [2]*Department of Anesthesiology, Vanderbilt University, Nashville, TN 37232, USA,* [3]*Molecular Physiology Unit, Department of Nephrology and Mineral Metabolism, Instituto Nacional de la Nutrición Salvador Zubirán, Instituto de Investigaciones Biomédicas UNAM, Mexico City, Mexico* and [4]*Department of Nephrology, Hospital Clinic, IDIBAPS, Universidad de Barcelona, Barcelona, Spain*

*Author for correspondence (e-mail: steven.hebert@mcmail.vanderbilt.edu)

Accepted 15 April; published on WWW 25 June 1998

Summary

Electroneutral cation–chloride cotransporters are widely expressed and perform a variety of physiological roles. A novel gene family of five members, encompassing a Na^+–Cl^- transporter, two Na^+–K^+–$2Cl^-$ transporters and two K^+–Cl^- cotransporters, encodes these membrane proteins; homologous genes have also been identified in a prokaryote and a number of lower eukaryotes. The cotransporter proteins share a common predicted membrane topology, with twelve putative transmembrane segments flanked by long hydrophilic N- and C-terminal cytoplasmic domains. The molecular identification of these transporters has had a significant impact on the study of their function, regulation and pathophysiology.

Key words: membrane protein, Na^+–K^+–$2Cl^-$ cotransport, Na^+–Cl^- cotransport, K^+–Cl^- cotransport, cotransport, bumetanide, furosemide, thiazide, kidney, choroid plexus, neuron, Gitelman's syndrome, Bartter's syndrome, macula densa, thick ascending limb of Henle, distal convoluted tubule.

Introduction

Electroneutral, diuretic-sensitive cotransport of Na^+, K^+ and Cl^- was first described in Ehrlich cells by Geck *et al.* (1980). The basic characteristics of this transport activity include a sensitivity to loop diuretics (most frequently bumetanide and furosemide), a stoichiometry of $1Na^+$:$1K^+$:$2Cl^-$ and a dependence on the simultaneous presence of all three transported ions. These functional criteria have been extremely useful, facilitating the identification of bumetanide-sensitive Na^+–K^+–$2Cl^-$ transport in a large number of cells and tissues (Kaplan *et al.* 1996*a*). Inwardly directed bumetanide-sensitive Na^+–K^+–$2Cl^-$ transport is activated by cell shrinkage, implicating this transporter in regulatory volume increase (Hoffmann and Dunham, 1995). In contrast, regulatory volume decrease invokes an outwardly directed Na^+-independent K^+–Cl^- cotransport activity which is weakly inhibited by bumetanide and furosemide (Lauf *et al.* 1992; Hoffmann and Dunham, 1995). A third distinct cation–chloride cotransporter, thiazide-sensitive Na^+–Cl^- transport, is abundant in the renal distal convoluted tubule (DCT) (Costanzo, 1985) and the flounder urinary bladder (Stokes, 1989). The cloning of all three classes of cation–chloride cotransporters has been accomplished over the last 4 years, resulting in the identification of a new five-member gene family (see Tables 1, 2). This review summarizes the subsequent advances in the molecular physiology of the vertebrate cation–chloride transporters.

Cloning of the cation–chloride transporters

The first cation–chloride transporter to be characterized at the molecular level was the thiazide-sensitive Na^+–Cl^- cotransporter from winter flounder (flTSC) (Gamba *et al.* 1993). A 3.7 kilobase flTSC cDNA was isolated by expression cloning in *Xenopus laevis* oocytes, using flounder urinary bladder as the source of poly(A)+ RNA. The expression of flTSC in *Xenopus laevis* oocytes produces a thiazide-sensitive Na^+–Cl^- transport with identical kinetics to that of the endogenous transporter. A cDNA encoding the first bumetanide-sensitive Na^+–K^+–$2Cl^-$ transporter was also cloned from a fish tissue, in this case shark rectal gland (Xu *et al.* 1994). This cDNA, termed NKCC1 (*N*a^+–*K*$^+$–*C*l^- *C*otransporter-1), was obtained by screening a shark cDNA library with two monoclonal antibodies specific for the purified bumetanide-binding protein. Functional expression in HEK-293 cells revealed the expected characteristics of a Na^+–K^+–$2Cl^-$ transporter, i.e. bumetanide-sensitive uptake of $^{86}Rb^+$ (a substitute for K^+) that was dependent on the presence of both Na^+ and Cl^-.

Table 1. *The five vertebrate cation–chloride transporters*

Cotransporter	Alternative nomenclature	Species	Size (number of amino acids)	Chromosome	GenBank number
TSC	NCC, SLC12A3	Flounder	1023		L11615
		Rat	1002		U10097
		Human	1021 (splice)	16q13	U44128
		Mouse	1002	8	U61085
		Rabbit	1028		AF028241
BSC1	NKCC2, SLC12A1	Rat	1095		U10096
		Rabbit	1099		U07547
		Mouse	1095	2	U94518
			770 (splice)		U61381
		Human	1099	16	U58130
BSC2	NKCC1, SLC12A2	Shark	1191		U05958
		Mouse	1205	18	U13174
		Human	1212	5q23.3	U30246
		Cow	1201		U70138
KCC1		Human	1085	16q22.1	U55054
		Rat	1085		U55815
		Rabbit	1085		U55053
		Pig	1086		AF028807
KCC2		Rat	1116		U55816

BSC1 and BSC2 encode bumetanide-sensitive Na^+–K^+–$2Cl^-$ cotransporters, TSC encodes a thiazide-sensitive Na^+–Cl^- cotransporter, and KCC1 and KCC2 encode K^+–Cl^- cotransporters. Molecular size denotes the open-reading frames predicted from cDNA sequences.

The fish cDNA clones were subsequently utilized to identify the mammalian homologs of the electroneutral cation–chloride transporters (Table 1). A fragment of the flTSC cDNA was used to 'fish' out cDNAs encoding the rat thiazide-sensitive cotransporter (rTSC) and apical bumetanide-sensitive Na^+–K^+–$2Cl^-$ transporter (rBSC1) from renal cortex and outer medulla, respectively (Gamba *et al.* 1994). Mouse BSC1 cDNAs (NKCC2 in the alternative nomenclature) have also been identified (Mount *et al.* 1995; Igarashi *et al.* 1995). All the full-length rodent TSC and BSC1 clones direct expression of the appropriate transport activity in *Xenopus* oocytes (Gamba *et al.* 1994). The mammalian NKCC1/BSC2 cotransporters have been cloned using similar homology-based approaches (Delpire *et al.* 1994; Payne *et al.* 1995).

The two K^+–Cl^- cotransporter cDNAs were obtained through the identification of related human ESTs (expressed sequence tags) in the GenBank database. Several ESTs in the database were found to be moderately homologous to NKCC1, suggestive of a new branch of the cotransporter family. Using this information, and a combination of library screening and reverse transcriptase/polymerase chain reaction (RT-PCR), KCC1 cDNAs (K^+–Cl^- *C*otransporter-1) were subsequently isolated from rat, human and rabbit (Gillen *et al.* 1996). A

Table 2. *Full-length invertebrate cation–chloride transporters*

Species	Size (number of amino acids)	Locus	Accession number
Saccharomyces cerevisiae (yeast)	1120	YB5_yeast (SP)	P38329 (SP)
Nicotania tabacum (tobacco)	990	AF021220 (GB)	AF021220 (GB)
Manduca sexta (tobacco hornworm)	1060	MSU17344 (GB)	U17344 (GB) Q25479 (SP)
Caenorhabditis elegans (nematode)	1003 1020 952	CEL13A1 (GB) YRD_CAEEL (SP) CELT04B8 (GB)	U40798 (GB) Q09573 (SP) AF040650 (GB)

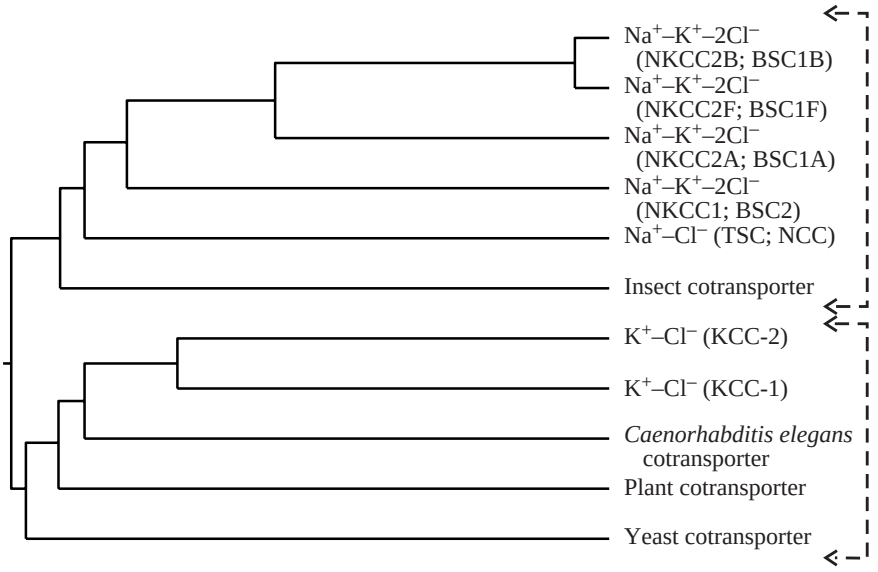

Fig. 1. The electroneutral cation–chloride cotransporter family; a homology tree of representative cotransporters based on amino acid sequences. The two main branches of the gene family are outlined. The length of the horizontal lines approximates evolutionary distance. Generated using the DNAStar program (Madison, WI, USA).

similar protocol resulted in the isolation of another putative K^+–Cl^- cotransporter, KCC2, from rat brain (Payne *et al.* 1996). Heterologous expression of both KCC1 and KCC2 fulfills the criteria for a K^+–Cl^- cotransporter (see below).

The percentage homology between the five mammalian cotransporters is shown in Fig. 2B. In addition to the multiple vertebrate cDNAs, putative cation–chloride cotransporter cDNAs and/or ESTs have been characterized from *Manduca sexta*, *Drosophila melanogaster*, *Caenorhabditis elegans*, yeast and a cyanobacterium (see Table 2 for selected full-length invertebrate homologs). A homology tree (Fig. 1) indicates the phylogenetic relationships between representative sequences, both vertebrate and invertebrate. Two main branches of the gene family can be appreciated, one consisting of predominantly renal Na^+-coupled cotransporters and the other of the K^+–Cl^- cotransporters and homologs from simpler organisms. All the cotransporter proteins share a basic structural motif, predicted by hydropathy analysis of their amino acid sequence (Fig. 2A). This primary structure predicts 12 putative hydrophobic transmembrane (TM) segments flanked by long hydrophilic N- and C-terminal cytoplasmic domains. Homology between family members is strongest within the TM domains, but is also evident in the C-terminal domains and in the predicted intracellular loops between TM segments. Human–shark BSC2 chimeras have demonstrated that the transport characteristics (affinities for Na^+, K^+, Cl^- and bumetanide) are encoded by the central 12 transmembrane domains (Isenring and Forbush, 1997). In the Na^+-dependent transporters (TSC, BSC1 and BSC2), there is a large extracellular loop between TM-7 and TM-8, with potential sites for N-linked glycosylation. An obvious structural departure is evident in the KCC1 and KCC2 sequences, which predict a glycosylated extracellular loop between TM-5 and TM-6 (Gillen *et al.* 1996; Payne *et al.* 1996). Full confirmation of the proposed membrane topology has yet to be published. However, both the N-terminal and C-terminal domains of shark BSC2 are clearly phosphorylated, indicating a cytoplasmic orientation (Lytle and Forbush, 1992; Xu *et al.* 1994). In addition, mutation of the first of two N-glycosylation sites in rTSC dramatically reduces glycosylation of the protein, confirming that the loop between TM-7 and TM-8 is extracellular (Poch *et al.* 1996).

Individual cotransporters

BSC1: Na^+–K^+–$2Cl^-$ cotransport

The renal thick ascending limb of the loop of Henle (TALH) is the main pharmacological target of the loop diuretics (bumetanide, ethacrynic acid, furosemide, piretanide and torsemide). These drugs exert their natriuretic effect by inhibition of electroneutral Na^+–K^+–$2Cl^-$ cotransport in the TALH (Greger, 1985). In contrast to secretory epithelia, which generally exhibit basolateral bumetanide-sensitive Na^+–K^+–$2Cl^-$ transport, this transport activity is located on the apical membrane of the TALH facing the tubule lumen (see Figs 3, 4). Bumetanide-sensitive Na^+–K^+–$2Cl^-$ cotransport in the TALH is encoded by BSC1/NKCC2 (hereafter referred to as BSC1), whereas bumetanide-sensitive Na^+–K^+–$2Cl^-$ transport elsewhere is the function of BSC2/NKCC1 (hereafter referred to as BSC2).

BSC1 plays a primary role in transcellular absorption of Na^+–Cl^- by the medullary and cortical TALH, and plays a secondary role in the paracellular transport of Na^+, Ca^{2+} and Mg^{2+} by this nephron segment (Greger, 1985; Hebert, 1992) (see below). Salt absorption by the TALH is crucial to countercurrent multiplication in the renal medulla and the excretion of a concentrated urine. The TALH also has a function in renal acid excretion, since NH_4^+ can substitute for K^+ in transport by BSC1 (Good, 1994). Ammonium generated by the renal proximal tubule is thus reabsorbed from the tubule lumen in the TALH and excreted from the renal interstitium by more distal nephron segments.

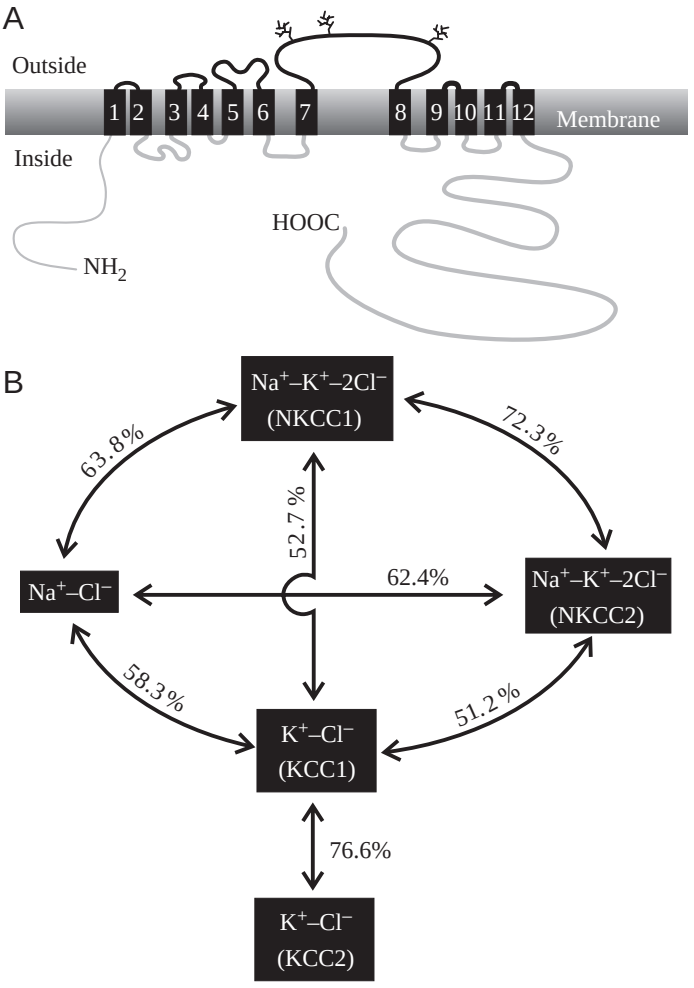

Fig. 2. (A) Predicted membrane topology of the Na^+-coupled cation–chloride cotransporters (BSC1/NKCC2, BSC2/NKCC1 and TSC/NCC). Analysis of amino acid sequences predicts a total of 12 transmembrane (TM) segments, flanked by large intracellular amino- and carboxy-terminal domains; there is a large predicted extracellular loop between TM-7 and TM-8. The KCC sequences predict a large extracellular loop between TM-5 and TM-6. (B) Diagram showing the percentage homology between the four human cation–chloride transporter proteins and rat KCC2.

Regulation of salt transport in the TALH, which is endowed with receptors for a large number of hormones, occurs through a combination of both primary and secondary effects on apical Na^+–K^+–$2Cl^-$ transport (Kaplan *et al.* 1996*a*). A number of hormones activate protein kinase A (PKA) in this nephron segment, resulting in an increase in salt transport. The primary structure of BSC1 predicts phosphorylation sites for both PKA and protein kinase C (PKC) (Gamba *et al.* 1994; Igarashi *et al.* 1995). Alternative splicing of the 3′ end of mouse BSC1 also modifies the predicted phosphorylation of the transporter protein by truncating the C terminus and substituting a unique C-terminal 55 amino acid segment (Mount *et al.* 1995). However, the functional significance of this alternative splicing is still unclear, and there is as yet no direct biochemical evidence for phosphorylation of any isoforms of BSC1.

In the mouse medullary TALH, vasopressin activates a switch in the K^+-dependence of apical Na^+–(K^+)–$2Cl^-$ transport, from a K^+-independent Na^+–Cl^- transporter to a K^+-dependent Na^+–K^+–$2Cl^-$ transporter (Sun *et al.* 1991). This modulation of apical Na^+–K^+–$2Cl^-$ transport is probably of crucial importance for the physiology of the TALH. Recycling of K^+ through the Na^+–K^+–$2Cl^-$ transporter and apical K^+ channels generates a lumen-positive potential difference, which drives the absorption of cations through a cation-selective paracellular pathway. This mechanism is responsible for the reabsorption of divalent cations (Ca^{2+} and Mg^{2+}) by the TALH (Greger, 1985; Hebert, 1992). In addition, the availability of a paracellular pathway for Na^+ doubles Na^+–Cl^- transport by the TALH without an increase in energy expenditure (Sun *et al.* 1991). K^+-independent bumetanide-sensitive Na^+–Cl^- transport has also been found in rabbit and rat TALH (Alvo *et al.* 1985; Ludens *et al.* 1995).

As predicted by its functional role, expression of BSC1 is restricted to the kidney, specifically the medullary and cortical TALH. Indeed, Tamm–Horsfall glycoprotein (Yu *et al.* 1994) and BSC1 (Igarashi *et al.* 1996) are the only known TALH-specific genes. Both BSC1 transcript (Gamba *et al.* 1994; Igarashi *et al.* 1995; Obermüller *et al.* 1996) and protein (Kaplan *et al.* 1996*c*; Ecelbarger *et al.* 1996) have been localized to the TALH. Affinity-purified antibodies to a C-terminal fusion protein of rBSC1 detect a protein of approximately 150 kDa in rat and mouse kidney (Kaplan *et al.* 1996*c*; Ecelbarger *et al.* 1996), the same size as the major renal bumetanide-binding protein (Haas *et al.* 1991). Immunofluorescence studies with this antibody label the apical membrane of all cells along the entire length of the TALH (Fig. 3A,C).

The availability of molecular probes for BSC1 and other transport proteins promises to refine significantly our understanding of the TALH phenotype. The low-conductance apical K^+ channel of the mammalian TALH is encoded by ROMK (rat outer medulla K^+ channel), the prototypical inwardly rectifying K^+ channel (Ho *et al.* 1993). Double-immunofluorescence studies with anti-ROMK and anti-BSC1 antibodies indicate a distinct heterogeneity of rat TALH, such that not all BSC1-positive TALH cells are positive for the ROMK protein (Xu *et al.* 1997). Electron microscopy of rat TALH has previously identified two subtypes of TALH cells, with both rough and smooth apical membranes differing in the abundance of apical microvilli (Allen and Tisher, 1976). In the hamster TALH, the relative frequency of these two cell types correlates closely with the proportion of cells having a high and low apical K^+ conductance (Tsuruoka *et al.* 1994), and the important issue of which morphological subtype of TALH cell expresses ROMK is under investigation.

Alternative splicing of BSC1 may also generate heterogeneity of ion transport in the TALH. Three mutually exclusive cassette exons have been described near the 5′ end

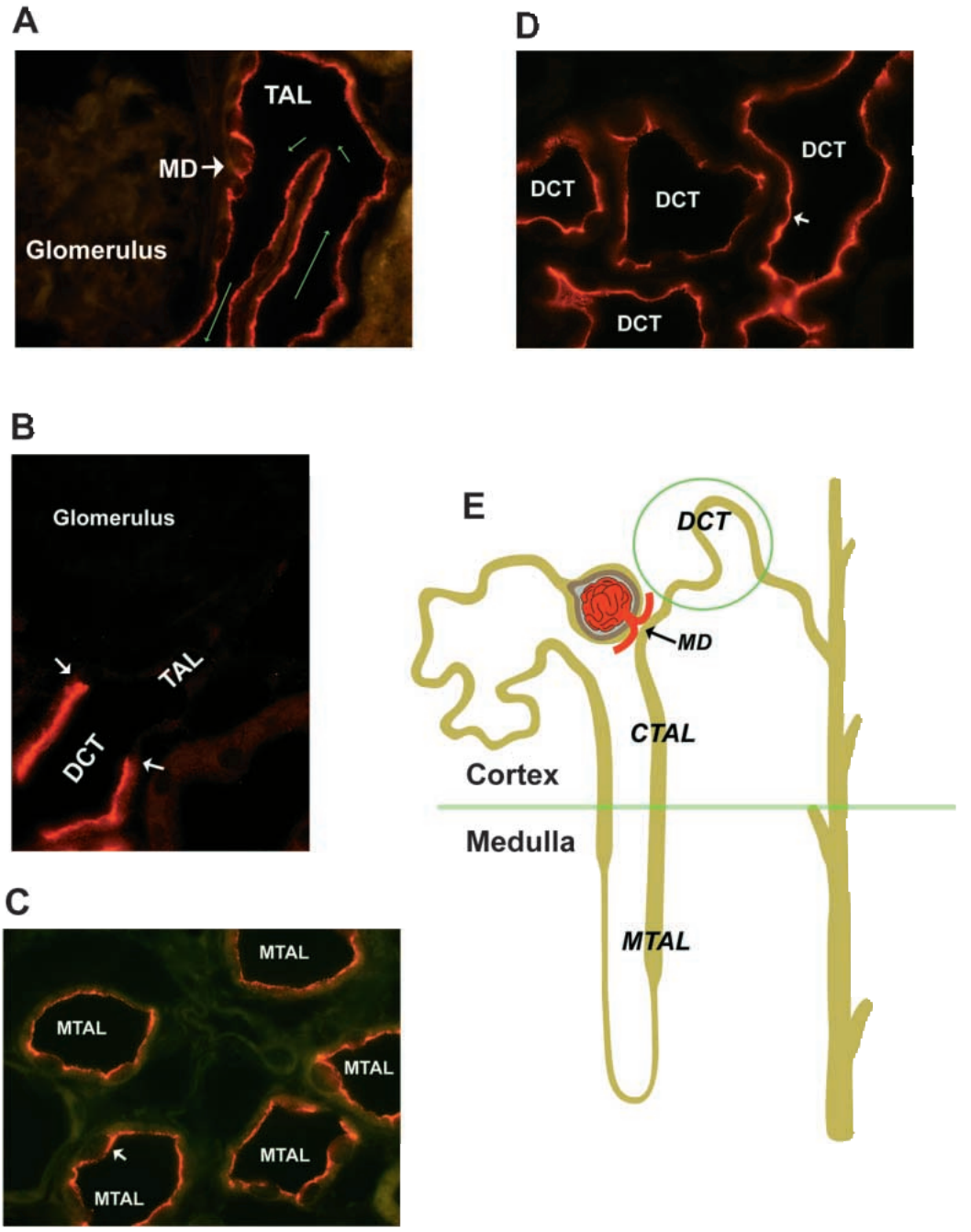

Fig. 3. Immunofluorescence of rat kidney, with antibodies to the kidney-specific cotransporters BSC1/NKCC2 and TSC/NCC. (A) Immunofluorescence (Rhodamine) with the anti-BSC1 antibody (Kaplan *et al.* 1996*c*). Red labelling of the apical membrane of the thick ascending limb (TAL) is seen. Apical labelling of taller columnar cells at the macula densa (MD) is also apparent. The green arrows indicate the direction of urine flow. (B) Immunofluorescence (Rhodamine) with the anti-TSC antibody (Plotkin *et al.* 1996). Labeling of distal tubule; arrows indicate the sharp border between the cortical TAL and the distal convoluted tubule (DCT). (C) Immunofluorescence of medullary TAL (MTAL) with the BSC1 antibody, clearly showing apical labeling (arrow). (D) Immunofluorescence of the DCT with anti-TSC antibody, showing apical labeling of cells (arrow). (E) Drawing of an idealized nephron, showing the cortical–medullary junction (green line) and the locations of medullary and cortical TAL (MTAL and CTAL), macula densa (MD) and distal convoluted tubule (DCT).

of rabbit, mouse and human BSC1 (Igarashi *et al.* 1995; Payne and Forbush, 1994; Mount *et al.* 1997). The cassette exons are predicted to encode 31 amino acids, spanning most of the second transmembrane domain and extending 10–13 amino acids into the cytoplasm. Expression of the individual cassettes is spatially restricted along the TALH, in the inner and outer stripe of outer medulla and in the cortical TALH (Igarashi *et al.* 1995; Payne and Forbush, 1994). The functional

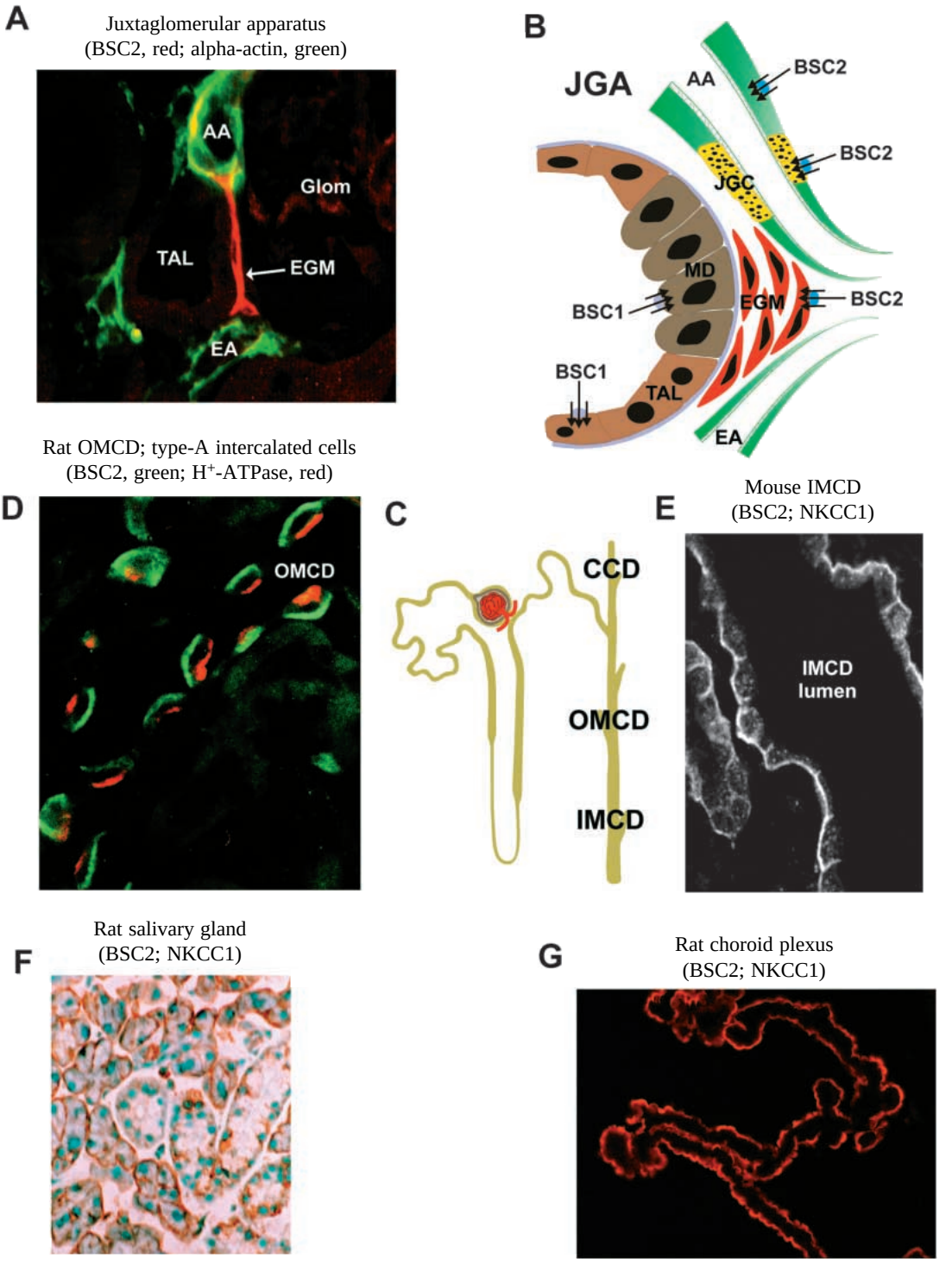

significance of this alternative splicing is not known. However, given the probable role of the transmembrane segments in ion binding and transport, it is highly likely that the cassette exons affect the relative affinity of apical cation–chloride transport along the TALH.

BSC1 protein (Kaplan *et al.* 1996*b*,*c*) and transcript (Obermüller *et al.* 1996) are also detected in the macula densa, a specialized group of tubular cells situated at the point of apposition of renal tubules with their parent glomeruli (Fig. 3A). The macula densa controls two important physiological processes, tubuloglomerular feedback and tubular regulation of renin release. An increase in luminal Na^+–Cl^- activity at the macula densa decreases glomerular filtration by inducing constriction of the afferent renal arteriole; this tubuloglomerular feedback mechanism is blocked by luminal furosemide (Ito and Carretero, 1990). Increases in

Fig. 4. Localization of BSC2/NKCC1 immunoreactivity in epithelial tissues (kidney, salivary gland and choroid plexus). (A) Co-staining of the mouse juxtaglomerular apparatus (kidney) with anti-BSC2 antibody (Kaplan *et al.* 1996*b*) and anti-α-actin antibody (a marker for vascular cells). Green (FITC staining) indicates cells staining only with anti-actin, red (Rhodamine) indicates cells labeled with anti-BSC2 alone, and areas of overlap are in yellow. A thin ribbon of BSC2-positive extraglomerular mesangial (EGM) cells is seen behind the macula densa and thick ascending limb (TAL). Light staining of the glomerulus (Glom) with anti-BSC2 is also evident. (B) A model of the juxtaglomerular apparatus (JGA), showing the relationships between cell types and transporters. Coloring follows the same pattern as in A. EGM, extraglomerular mesangial cells; MD, macula densa; AA, afferent arteriole; EA, efferent arteriole; JGC, juxtaglomerular cells; TAL, thick ascending limb of Henle. A subset of renin-negative (non-JG) cells in the afferent arteriole are BSC2-positive (Kaplan *et al.* 1996*b*). (C) A model of the nephron, showing the relative positions of the cortical collecting duct (CCD), outer medullary collecting duct (OMCD) and inner medullary collecting duct (IMCD). (D) Staining of type-A intercalated cells in rat outer medullary collecting duct (OMCD). The apical membrane stains with anti-H^+-ATPase antibody (red), a gift from Dr Stephen Gluck. The basolateral membrane stains with anti-BSC2 antibody (green). (E) Staining of mouse inner medullary collecting duct (IMCD) with anti-BSC2 antibody, clearly delineating the basolateral membranes. (F) Immunocytochemistry of rat salivary gland with anti-BSC2 antibody, indicating basolateral staining (brown) of epithelial cells. (G) Immunofluorescence of rat choroid plexus; apical membranes stain red with anti-BSC2 antibody.

luminal Na^+–Cl^- activity at the macula densa also inhibit renin release from juxtaglomerular cells in the afferent arteriole, an effect that is blocked by luminal bumetanide and furosemide (Lorenz *et al.* 1991). Macula densa cells have been shown to possess apical bumetanide-sensitive Na^+–K^+–$2Cl^-$ transport with a K_m for Cl^- of 32.5 mmol l^{-1} (Lapointe *et al.* 1995). This K_m is close to the half-maximal concentration of tubular Cl^- for inhibition of renin release (He *et al.* 1995). Indeed, it appears that the macula densa responds to changes in tubular Cl^- concentration, since variations in tubular Na^+ concentration have no effect on tubuloglomerular feedback or renin secretion (Lorenz *et al.* 1991).

BSC2: Na^+–K^+–$2Cl^-$ cotransport

Bumetanide-sensitive Na^+–K^+–$2Cl^-$ transport is a feature of perhaps all cultured mammalian cells. However, recent developments suggest that data from tissue-specific cell lines cannot be extrapolated to native tissue, since a number of cell types which express bumetanide-sensitive Na^+–K^+–$2Cl^-$ transport in culture do not appear to express BSC2 *in vivo* (Kaplan *et al.* 1996*b*; Plotkin *et al.* 1997*a*). BSC2 transcript and transport activity are not detected in freshly isolated proximal tubule cells, aortic endothelial cells and vascular smooth muscle cells, but are induced after more prolonged culture (Raat *et al.* 1996). Although low-level expression of BSC2 protein is detectable in freshly isolated endothelial cells (Yerby *et al.* 1997), evidence for *in vivo* expression in this cell type has not been published. Induction of BSC2 in culture may be involved in the increase in cell volume necessary for cell growth and progression through the cell cycle. In NIH 3T3 cells, for example, K^+ content and cell volume increase after serum stimulation, and bumetanide has an anti-proliferative effect (Bussolati *et al.* 1996). The influx of Na^+ through amiloride- and bumetanide-sensitive pathways is also an early event after serum stimulation of 3T3 cells (Berman *et al.* 1995).

A more direct role for cation–chloride transporters in cell growth and signal transduction is suggested by genetic manipulation of tobacco protoplasts (Harling *et al.* 1997). One of several auxin-independence genes isolated by activation T-DNA tagging, *axi-4*, encodes a plant protein with significant homology to cation–chloride cotransporters. Overexpression of full-length *axi-4* or shark NKCC1 in protoplasts confers auxin-independent cell growth. However, only a portion of the *axi-4* gene was isolated in the initial T-DNA tagging, and the C-terminal 237 amino acids of the axi-4 protein are sufficient to confer auxin-independent growth (Harling *et al.* 1997). This suggests that the C-terminal domains of the cation–chloride transporters, which share a moderate degree of homology, play a direct role in cellular growth.

The expression pattern of BSC2 in the kidney and the nervous system has been examined in detail (Kaplan *et al.* 1996*b*; Plotkin *et al.* 1997*a*). These studies utilized a polyclonal antibody specific for a C-terminal mBSC2 fusion protein. This antibody recognizes two proteins of approximately 145 kDa and 155 kDa, which are probably differentially glycosylated forms of BSC2. Within the brain, BSC2 transcript is most abundant in the choroid plexus, followed by the cerebellum and brain stem. Immunofluorescence and functional studies localize BSC2 to the apical cell membrane of the choroid plexus (Plotkin *et al.* 1997*a*) (Fig. 4G). The precise role of BSC2 in the choroid plexus is unclear. However, a component of cerebrospinal fluid production is bumetanide-sensitive (Javaheri and Wagner, 1993).

BSC2 protein is also detected in some neuronal cell bodies and dendrites in the brain and in dorsal root ganglion sensory neurons in the peripheral nervous system (Plotkin *et al.* 1997*a*). This observation is particularly important, since the magnitude of the Cl^- electrochemical gradient plays an important role in the response of neurons to stimuli that affect Cl^- conductance (Misgeld *et al.* 1986; Staley *et al.* 1996). In neurons with strong inward transport of Cl^-, intracellular Cl^- concentration is high and $GABA_A$ receptor stimulation, which activates a Cl^- channel, is depolarizing and excitatory. In contrast, in cells demonstrating outward Cl^- transport, $GABA_A$ activation is hyperpolarizing and inhibitory. Both inward and outward transport of Cl^- in neurons are diuretic-sensitive and are probably encoded by BSC2 and KCC1/KCC2 (see below), respectively. BSC2 in the central nervous system is developmentally regulated, with high levels of expression at birth and during the first few postnatal days, and decreased levels of expression thereafter (Plotkin *et al.* 1997*b*). This

correlates very well with the switch of the GABA effect, from depolarizing to hyperpolarizing, during the first weeks of postnatal life.

Within mouse kidney, heavy expression of BSC2 protein is detected at the basolateral membrane of inner medullary collecting duct cells (IMCD) (Kaplan *et al.* 1996*b*) (Fig. 4E). This result was expected, since there is *in vivo* evidence for hormone-sensitive basolateral Na^+–K^+–$2Cl^-$ transport in rodent IMCD (Rocha and Kudo, 1990). Within the glomerulus, light staining of mesangial cells is also evident (Fig. 4A). Cultured mesangial cells have a well-characterized Na^+–K^+–$2Cl^-$ transport system which is activated by factors such as angiotensin II (Homma and Harris, 1991). Unexpected staining of BSC2 is also found in juxtaglomerular cells in the afferent arteriole, suggesting a role in the regulation of renin secretion by these cells (Fig. 4A,B). The so-called 'extraglomerular' mesangial cells, located between the glomerulus and the macula densa, are also labeled with BSC2 antibody (Fig. 4A). The function of BSC2 in the glomerulus and juxtaglomerular apparatus is unknown. However, the dominant role of extracellular Cl^- in the function of the juxtaglomerular apparatus and associated cells is intriguing (Tsukahara *et al.* 1994; Matsunaga *et al.* 1994). As in neurons, BSC2 may modulate the transmembrane Cl^- gradient, altering the response of renal cells to agents that affect Cl^- conductance (Ling *et al.* 1995).

The distribution of BSC2 in rat kidney has also been studied, using the antibody described above (Fig. 4D) and an antibody generated against a C-terminal rat BSC2 peptide (Ginns *et al.* 1996). These studies replicate the findings in mouse kidney; however, cells within the rat IMCD are not labeled. In the rat outer medullary collecting duct, however, the basolateral membranes of type A intercalated cells are stained by the rBSC2 antibody (Ginns *et al.* 1996) (Fig. 4D). The type A intercalated cell, defined by expression of an apical H^+-ATPase and a basolateral Cl^-–HCO_3^- exchanger, functions in acid secretion (Brown and Breton, 1996). It has been demonstrated that basolateral BSC2 in a mouse IMCD cell line is capable of transporting NH_4^+ (Wall *et al.* 1995). Therefore, both BSC1 (see above) and BSC2 are part of the pathway for renal excretion of NH_4^+.

Within secretory epithelia, BSC2 protein has been localized to the basolateral membrane of acinar cells in rat submandibular gland (Fig. 4F) (He *et al.* 1997) and parotid gland (Lytle *et al.* 1995). Heterogeneous staining of the basolateral membrane of intralobular duct cells in submandibular gland has also been observed (He *et al.* 1997). BSC2 is heavily expressed in stomach, and the level of transcript in the *Necturus maculosus* gastric fundus essentially doubles after feeding (Soybel *et al.* 1995). Functional experiments in this model strongly support a role for BSC2 in the secretion of stomach acid, probably by providing a basolateral entry pathway for Cl^- (Soybel *et al.* 1995).

The complex functional regulation of BSC2 has previously been reviewed in detail (Haas, 1994; Kaplan *et al.* 1996*a*; Mount *et al.* 1997). Although all the cation–chloride transporters are predicted to be substrates for protein kinases, BSC2 is the only member of the family for which there is published evidence of phosphorylation (Xu *et al.* 1994; Tanimura *et al.* 1995; Plotkin *et al.* 1997*a*). The activation of PKA in rat parotid gland stimulates phosphorylation of one of at least three phosphorylation sites in the BSC2 protein, indicating a direct role for protein phosphorylation in the regulation of BSC2 (Tanimura *et al.* 1995). However, the modulation of BSC2 by PKA is evidently very complex, involving alternative splicing, secondary activation of other protein kinases and protein–protein interactions. The solitary predicted PKA site in BSC2 is encoded by a short exon that is removed by alternative splicing in several mouse tissues, such that a fraction of BSC2 is not predicted to be a substrate for PKA (Randall *et al.* 1997). In shark rectal gland, activation of PKA results in phosphorylation of BSC2 on a threonine that is not part of a consensus PKA site (Lytle and Forbush, 1992). This phosphorylation can be blocked by raising internal Cl^- concentration, suggesting that the effect of PKA is mediated by a Cl^--sensitive phosphorylation event that does not directly involve this kinase (Lytle and Forbush, 1996). Cl^- may thus regulate its own transport by affecting phosphorylation of BSC2, and this phenomenon has also been reported in mammalian epithelial cells (Haas *et al.* 1995). Finally, in the T84 cell line, BSC2 co-immunoprecipitates with two integral membrane proteins of 130 and 160 kDa. Activation of PKA increases the surface expression of these co-precipitated proteins, with a lesser effect on the surface expression of BSC2 (D'Andrea *et al.* 1996).

TSC: Na^+–Cl^- cotransport

In the distal convoluted tubule (DCT) of the mammalian kidney, the primary apical entry pathway for Na^+ is through the thiazide-sensitive Na^+–Cl^- cotransporter (Mount *et al.* 1997). The natriuretic effect of the thiazide diuretics underlies their therapeutic effect in edema states and hypertension. In addition, luminal thiazide in the DCT has a hypocalciuric effect, implicating TSC in the fine-tuning of Ca^{2+} excretion (Costanzo, 1985). Although microperfusion identified the DCT as the primary site of action of the thiazides, newer molecular probes have been invaluable in defining the phenotype of cells in this segment of the kidney. A TSC-specific antibody raised against an amino-terminal rTSC fusion protein detects the TSC protein at the apical cell membrane of the DCT (Fig. 3D). The transition between the BSC1-positive cells of the cortical TALH and the TSC-positive DCT is dramatic (Fig. 3B). However, in the rat and human kidney (Plotkin *et al.* 1996; Obermüller *et al.* 1995), the distal border of the DCT is less distinct, with a mixture of TSC-negative and TSC-positive cells in the connecting segment between the DCT and the cortical collecting duct. Consistent with the role of TSC in Ca^{2+} homeostasis, all cells that express this transporter in the DCT and beyond are also positive for calbindin D28 (Plotkin *et al.* 1996), an intracellular Ca^{2+}-binding protein implicated in transcellular Ca^{2+} transport.

KCC1 and KCC2: K^+–Cl^- cotransport

Electroneutral cotransport of K^+–Cl^- is detected in a wide range of cells functioning in regulatory volume decrease, transepithelial salt transport and the maintenance of transmembrane Cl^- gradients. Consistent with this broad functional distribution, KCC1 transcript is heavily expressed in many tissues, including brain (Gillen *et al.* 1996). Precise localization awaits the development of a KCC1-specific antibody. In contrast to KCC1, KCC2 expression is restricted to the brain, and *in situ* hybridization reveals KCC2 transcript in neurons throughout the central nervous system (Payne *et al.* 1996). A BLAST search of the EST database with rKCC2 also detects a significant number of related ESTs in a cDNA library from human retina (D. B. Mount, unpublished results).

Stable expression of full-length rabbit KCC1 in HEK-293 cells reveals the expected characteristics of a K^+–Cl^- cotransporter (Lauf *et al.* 1992): $^{86}Rb^+$ efflux in these cells is stimulated by cell swelling to a much greater extent than in untransfected cells. Cl^--dependent influx of $^{86}Rb^+$ in stable transfectants is activated by treatment with *N*-ethylmaleimide (NEM), a reagent that probably exerts its effect by modification of sulfhydryl groups on the transporter and/or associated proteins. This influx is weakly furosemide- and bumetanide-sensitive (Gillen *et al.* 1996), and kinetic analysis also indicates a low affinity of the transporter for both K^+ (K_m>25 mmol l^{-1}) and Cl^- (K_m>50 mmol l^{-1}).

In contrast to KCC1, stable expression of KCC2 in HEK-293 cells results in a K^+–Cl^- cotransporter which is not activated by cell swelling (Payne, 1997). KCC2 also displays a much higher affinity for extracellular K^+ (K_m≈5.2 mmol l^{-1}). On the basis of thermodynamic considerations, KCC2 may function in the buffering of external K^+ within the central nervous system, in addition to maintaining the transmembrane Cl^- gradient (Payne, 1997).

K^+–Cl^- cotransport in red blood cells is stimulated by kinase inhibition and inactivated by phosphatase inhibition (Flatman *et al.* 1996; Lauf *et al.* 1992). Genetic evidence has recently implicated the cytoplasmic tyrosine kinases Fgr and Hck in the regulation of erythrocyte K^+–Cl^- cotransport (De Franceschi *et al.* 1997). Thus, red cell K^+ content is lower in $fgr^{-/-}hck^{-/-}$ mice owing to an activation of K^+–Cl^- cotransport. Okadaic acid is capable of inhibiting K^+–Cl^- cotransport in double-negative red cells, suggesting that the Fgr and Hck tyrosine kinases negatively regulate a phosphatase, which in turn inhibits KCC1.

Pathophysiology of cation–chloride cotransport

Given the physiological importance of both thiazide- and bumetanide-sensitive salt transport by the kidney, it is not surprising that altered activity of these transporters has been implicated in human disease. Even before the availability of cDNA clones, the human BSC1 and TSC genes were leading candidate loci for two forms of inherited metabolic alkalosis, Bartter's syndrome and Gitelman's syndrome (Stein, 1985). In addition to a hypokalemic alkalosis, patients with Bartter's syndrome have a decreased urinary concentrating ability and polyuria, and generally exhibit increased urinary excretion of Ca^{2+} with a normal serum Mg^{2+} level (Bettinelli *et al.* 1992). This constellation of findings is most compatible with a primary defect in the TALH. As anticipated, mutations in the human BSC1 gene have recently been reported in several kindreds with Bartter's syndrome (Simon *et al.* 1996*a*). However, other families with Bartter's syndrome do not exhibit linkage to BSC1, suggesting genetic heterogeneity. Mutations in the human ROMK K^+ channel gene have also been identified in families with Bartter's syndrome (Simon *et al.* 1996*b*; International Collaborative Study Group, 1997), underscoring the functional coupling between apical K^+ channels and apical Na^+–K^+–$2Cl^-$ transport in the mammalian TALH. More recently, a third gene, CLC-KNB, has been implicated in the genesis of Bartter's syndrome in a third subset of families with the disease (Simon *et al.* 1997). CLC-KNB is a member of the CLC family of Cl^- channels and probably encodes a component of the basolateral Cl^- conductance in TALH cells.

In contrast to Bartter's syndrome, patients with Gitelman's syndrome do not have a defect in urinary concentrating ability. Another major distinguishing feature is the presence of marked hypomagnesemia and hypocalcuria in Gitelman's syndrome (Bettinelli *et al.* 1992). The primary defect in this syndrome appears to be in the distal tubule, and the lack of a diuretic response to thiazides in some patients pointed to mutations in TSC. Linkage of the human TSC gene to Gitelman's syndrome has recently been reported, along with the direct characterization of non-conservative mutations in affected patients (Simon *et al.* 1996*c*; Mastroianni *et al.* 1996; Lemmink *et al.* 1996; Takeuchi *et al.* 1996; Pollak *et al.* 1996).

The other cation–chloride cotransporter genes are not obvious candidates for monogenic disorders, but probably play a role in human disease. For example, excessive K^+–Cl^- cotransport and cellular dehydration may underlie the destruction of red cells in hemolytic anemias, particularly in sickle cell anemia (Franco *et al.* 1995). In addition, the importance of the transmembrane Cl^- gradient in neuronal excitability implicates BSC2 and the K^+–Cl^- cotransporters in seizure disorders (Hochman *et al.* 1995; Payne, 1997).

Conclusions

The cloning of the cation–chloride transporters was a significant advance and has already begun to clarify a previously confusing field. It is highly likely that other members of this rapidly expanding gene family remain to be discovered. Localization studies have been informative, and the cotransporter antibodies are proving to be valuable phenotypic and functional markers. The ability to specifically inhibit individual genes by both germline inactivation and anti-sense technology should help clarify some of the remaining physiological issues, such as the roles of BSC1 and BSC2 in tubuloglomerular feedback and tubular regulation of renin release. Within cells, the C termini of cation–chloride

transporters may play a fundamental role in the regulation of cell growth, independent of the effect of cation–chloride cotransport on intracellular ion concentrations (Harling *et al.* 1997). Conversely, the level of intracellular Na^+ and K^+ modulates the activation of apoptosis; the role of the cation–chloride transporters in this process is not known and is an intriguing area for future investigation (Bortner *et al.* 1997; Hughes *et al.* 1997). At the molecular level, the identification of ion translocation sites, phosphorylation sites and transporter-associated proteins is pending. This information will help resolve issues such as the differences in ionic affinity between transporters (Payne *et al.* 1995; Payne, 1997; Isenring and Forbush, 1997) and the inverse effect of kinases, phosphatases and cell volume on the activity of BSC2 and KCC1 (Hoffmann and Dunham, 1995).

Original research was supported by grants from the National Institues of Health to S.C.H. (DK45792 and DK36803), to D.B.M. (DK02328) and to E.D. (HL49251) and from the Mexican Council of Science and Technology to G.G. (CONACYT, M3840). E.D. is an Established Investigator of the American Heart Association and G.G. is an International Research Scholar of the Howard Hughes Medical Institute.

References

ALLEN, F. AND TISHER, C. C. (1976). Morphology of the ascending thick limb of Henle. *Kidney Int.* **9**, 8–22.

ALVO, M., CALAMIA, J. AND EVELOFF, J. (1985). Lack of potassium effect on Na^+–Cl^- cotransport in the medullary thick ascending limb. *Am. J. Physiol.* **249**, F34–F39.

BERMAN, E., SHARON, I. AND ATLAN, H. (1995). An early transient increase of intracellular Na^+ may be one of the first components of the mitogenic signal. Direct detection by $^{23}Na^+$-NMR spectroscopy in quiescent 3T3 mouse fibroblasts stimulated by growth factors. *Biochim. biophys. Acta* **1239**, 177–185.

BETTINELLI, A., BIANCHETTI, M. G., GIRARDIN, E., CARINGELLA, A., CECCONI, M., APPIANI, A. C., PAVANELLO, L., GASTALDI, R., ISIMBALDI, C., LAMA, G., MARCHESONI, C., MATTEUCI, C., PATRIACCA, P., DI NATALE, B., SETZU, C. AND VITUCCI, P. (1992). Use of calcium excretion values to distinguish two forms of primary renal tubular hypokalemic alkalosis: Bartter and Gitelman syndromes. *J. Pediatr.* **120**, 38–43.

BORTNER, C. D., HUGHES, F. M. J. AND CIDLOWSKI, J. A. (1997). A primary role for K^+ and Na^+ efflux in the activation of apoptosis. *J. biol. Chem.* **272**, 32436–32442.

BROWN, D. AND BRETON, S. (1996). Mitochondria-rich, proton-secreting epithelial cells. *J. exp. Biol.* **199**, 2345–2358.

BUSSOLATI, O., UGGERI, J., BELLETTI, S., DALL'ASTA, V. AND GAZZOLA, G. C. (1996). The stimulation of Na^+,K^+,Cl^- cotransport and of system A for neutral amino acid transport is a mechanism for cell volume increase during the cell cycle. *FASEB J.* **10**, 920–926.

COSTANZO, L. S. (1985). Localization of diuretic action in microperfused rat distal tubules: Ca^{2+} and Na^+ transport. *Am. J. Physiol.* **248**, F527–F535.

D'ANDREA, L., LYTLE, C., MATTHEWS, J. B., HOFMAN, P., FORBUSH III, B. R. AND MADARA, J. L. (1996). Na^+–K^+–$2Cl^-$ cotransporter (NKCC) of intestinal epithelial cells. Surface expression in response to cyclic AMP. *J. biol. Chem.* **271**, 28969–28976.

DE FRANCESCHI, L., FUMAGALLI, L., OLIVIERI, O., CORROCHER, R., LOWELL, C. A. AND BERTON, G. (1997). Deficiency of Src family kinases Fgr and Hck results in activation of erythrocyte K^+–Cl^- cotransport. *J. clin. Invest.* **99**, 220–227.

DELPIRE, E., RAUCHMAN, M. I., BEIER, D. R., HEBERT, S. C. AND GULLANS, S. R. (1994). Molecular cloning and chromosome localization of a putative basolateral Na^+–K^+–$2Cl^-$ cotransporter from mouse inner medullary collecting duct (mIMCD-3) cells. *J. biol. Chem.* **269**, 25677–25683.

ECELBARGER, C. A., TERRIS, J., HOYER, J. R., NIELSEN, S., WADE, J. B. AND KNEPPER, M. A. (1996). Localization and regulation of the rat renal Na^+–K^+–$2Cl^-$ cotransporter, BSC-1. *Am. J. Physiol.* **271**, F619–F628.

FLATMAN, P. W., ADRAGNA, N. C. AND LAUF, P. K. (1996). Role of protein kinases in regulating sheep erythrocyte K^+–Cl^- cotransport. *Am. J. Physiol.* **271**, C255–C263.

FRANCO, R. S., PALASCAK, M., THOMPSON, H. AND JOINER, C. H. (1995). K^+–Cl^- cotransport activity in light *versus* dense transferrin receptor-positive sickle reticulocytes. *J. clin. Invest.* **95**, 2573–2580.

GAMBA, G., MIYANOSHITA, A., LOMBARDI, M., LYTTON, J., LEE, W. S., HEDIGER, M. A. AND HEBERT, S. C. (1994). Molecular cloning, primary structure and characterization of two members of the mammalian electroneutral sodium–(potassium)–chloride cotransporter family expressed in kidney. *J. biol. Chem.* **269**, 17713–17722.

GAMBA, G., SALTZBERG, S. N., LOMBARDI, M., MIYANOSHITA, A., LYTTON, J., HEDIGER, M. A., BRENNER, B. M. AND HEBERT, S. C. (1993). Primary structure and functional expression of a cDNA encoding the thiazide-sensitive, electroneutral sodium–chloride cotransporter. *Proc. natn. Acad. Sci. U.S.A.* **90**, 2749–2753.

GECK, P., PIETRZYK, C., BURCKHARDT, B. C., PFEIFFER, B. AND HEINZ, E. (1980). Electrically silent cotransport on Na^+, K^+ and Cl^- in Ehrlich cells. *Biochim. biophys. Acta* **600**, 432–447.

GILLEN, C. M., BRILL, S., PAYNE, J. A. AND FORBUSH III, B. (1996). Molecular cloning and functional expression of the K^+–Cl^- cotransporter from rabbit, rat and human. A new member of the cation–chloride cotransporter family. *J. biol. Chem.* **271**, 16237–16244.

GINNS, S. M., KNEPPER, M. A., ECELBARGER, C. A., TERRIS, J., HE, X., COLEMAN, R. A. AND WADE, J. B. (1996). Immunolocalization of the secretory isoform of Na^+–K^+–Cl^- cotransporter in rat renal intercalated cells. *J. Am. Soc. Nephrol.* **7**, 2533–2542.

GOOD, D. W. (1994). Ammonium transport by the thick ascending limb of Henle's loop. *A. Rev. Physiol.* **56**, 623–647.

GREGER, R. (1985). Ion transport mechanisms in thick ascending limb of Henle's loop of mammalian nephron. *Physiol. Rev.* **65**, 760–797.

HAAS, M. (1994). The Na^+–K^+–Cl^- cotransporters. *Am. J. Physiol.* **267**, C869–C885.

HAAS, M., DUNHAM, P. B. AND FORBUSH, B. R. (1991). [^{3}H]-bumetanide binding to mouse kidney membranes: identification of corresponding membrane proteins. *Am. J. Physiol.* **260**, C791–C804.

HAAS, M., MCBRAYER, D. AND LYTLE, C. (1995). $[Cl^-]_i$-dependent phosphorylation of the Na^+–K^+–Cl^- cotransport protein of dog tracheal epithelial cells. *J. biol. Chem.* **270**, 28955–28961.

HARLING, H., CZAJA, I., SCHELL, J. AND WALDEN, R. (1997). A plant cation–chloride co-transporter promoting auxin-independent tobacco protoplast division. *EMBO J.* **16**, 5855–5866.

He, X.-R., Greenberg, S. G., Briggs, J. P. and Schnermann, J. (1995). Effects of furosemide and verapamil on the Na^+,Cl^- dependency of macula densa-mediated renin secretion. *Hypertension* **26**, 137–142.

He, X., Tse, C. M., Donowitz, M., Alper, S. L., Gabriel, S. E. and Baum, B. J. (1997). Polarized distribution of key membrane transport proteins in the rat submandibular gland. *Pflügers Arch.* **433**, 260–268.

Hebert, S. C. (1992). Nephron heterogeneity. In *Handbook of Physiology – Renal Physiology*, vol. 1, chapter 20, pp. 875–925. Oxford: Oxford University Press.

Ho, K., Nichols, C. G., Lederer, W. J., Lytton, J., Vassilev, P. M., Kanazirska, M. V. and Hebert, S. C. (1993). Cloning and expression of an inwardly rectifying ATP-regulated potassium channel. *Nature* **362**, 31–38.

Hochman, D. W., Baraban, S. C., Owens, J. W. and Schwartzkroin, P. A. (1995). Dissociation of synchronization and excitability in furosemide blockade of epileptiform activity. *Science* **270**, 99–102.

Hoffmann, E. K. and Dunham, P. B. (1995). Membrane mechanisms and intracellular signalling in cell volume regulation. *Int. Rev. Cytol.* **161**, 173–262.

Homma, T. and Harris, R. C. (1991). Time-dependent biphasic regulation of Na^+–K^+–Cl^- cotransport in rat glomerular mesangial cells. *J. biol. Chem.* **266**, 13553–13559.

Hughes, F. M. J., Bortner, C. D., Purdy, G. D. and Cidlowski, J. A. (1997). Intracellular K^+ suppresses the activation of apoptosis in lymphocytes. *J. biol. Chem.* **272**, 30567–30576.

Igarashi, P., Vanden Heuvel, G. B., Payne, J. A. and Forbush III, B. (1995). Cloning, embryonic expression and alternative splicing of a murine kidney-specific Na^+–K^+–Cl^- cotransporter. *Am. J. Physiol.* **269**, F405–F418.

Igarashi, P., Whyte, D. A., Li, K. and Nagami, G. T. (1996). Cloning and kidney cell-specific activity of the promoter of the murine renal Na^+–K^+–Cl^- cotransporter gene. *J. biol. Chem.* **271**, 9666–9674.

International Collaborative Study Group (1997). Mutations in the gene encoding the inwardly-rectifying renal potassium channel, ROMK, cause the antenatal variant of Bartter syndrome: evidence for genetic heterogeneity. *Human molec. Genet.* **6**, 17–26.

Isenring, P. and Forbush III, B. (1997). Ion and bumetanide binding by the Na^+–K^+–Cl^- cotransporter. Importance of transmembrane domains. *J. biol. Chem.* **272**, 24556–24562.

Ito, S. and Carretero, O. A. (1990). An *in vitro* approach to the study of macula densa-mediated glomerular hemodynamics. *Kidney Int.* **38**, 1206–1210.

Javaheri, S. and Wagner, K. R. (1993). Bumetanide decreases canine cerebrospinal fluid production. *In vivo* evidence for Na^+–Cl^- cotransport in the central nervous system. *J. clin. Invest.* **92**, 2257–2261.

Kaplan, M. R., Mount, D. B., Delpire, E., Gamba, G. and Hebert, S. C. (1996*a*). Molecular mechanisms of Na^+,Cl^- cotransport. *A. Rev. Physiol.* **58**, 649–668.

Kaplan, M. R., Plotkin, M. D., Brown, D., Hebert, S. C. and Delpire, E. (1996*b*). Expression of the mouse Na^+–K^+–Cl^- cotransporter, mBSC2, in the terminal inner medullary collecting duct, the glomerular and extraglomerular mesangium and the glomerular afferent arteriole. *J. clin. Invest.* **98**, 723–730.

Kaplan, M. R., Plotkin, M. D., Lee, W. S., Xu, Z. C., Lytton, J. and Hebert, S. C. (1996*c*). Apical localization of the Na^+–K^+–Cl^- cotransporter, rBSC1, on rat thick ascending limbs. *Kidney Int.* **49**, 40–47.

Lapointe, J. Y., Laamarti, A., Hurst, A. M., Fowler, B. C. and Bell, P. D. (1995). Activation of Na^+–K^+–$2Cl^-$ cotransport by luminal chloride in macula densa cells. *Kidney Int.* **47**, 752–757.

Lauf, P. K., Bauer, J., Adragna, N. C., Fujise, H., Zade-Oppen, A. M., Ryu, K. H. and Delpire, E. (1992). Erythrocyte K^+–Cl^- cotransport: properties and regulation. *Am. J. Physiol.* **263**, C917–C132.

Lemmink, H. H., van den Heuvel, L. P., van Dijk, H. A., Merkx, G. F., Smilde, T. J., Taschner, P. E., Monnens, L. A., Hebert, S. C. and Knoers, N. V. (1996). Linkage of Gitelman syndrome to the thiazide-sensitive sodium–chloride cotransporter gene with identification of mutations in Dutch families. *Pediatric Nephrol.* **10**, 403–407.

Ling, B. N., Matsunaga, H., Ma, H. and Eaton, D. C. (1995). Role of growth factors in mesangial cell ion channel regulation. *Kidney Int.* **48**, 1158–1166.

Lorenz, J. N., Weihprecht, H., Schnermann, J., Skott, O. and Briggs, J. P. (1991). Renin release from isolated juxtaglomerular apparatus depends on macula densa chloride transport. *Am. J. Physiol.* **260**, F486–F493.

Ludens, J. H., Clark, M. A. and Lawson, J. A. (1995). Does ADH alter cotransporter properties in conscious rats?: evidence for a shift from K^+-independent to K^+-dependent cotransport. *J. Am. Soc. Nephrol.* **6**, 344.

Lytle, C. and Forbush III, B. (1992). The Na^+–K^+–Cl^- cotransport protein of shark rectal gland. II. Regulation by direct phosphorylation. *J. biol. Chem.* **267**, 25438–25443.

Lytle, C. and Forbush III, B. (1996). Regulatory phosphorylation of the secretory Na^+–K^+–Cl^- cotransporter: modulation by cytoplasmic Cl^-. *Am. J. Physiol.* **270**, C437–C448.

Lytle, C., Xu, J. C., Biemesderfer, D. and Forbush III, B. (1995). Distribution and diversity of Na^+–K^+–Cl^- cotransport proteins: a study with monoclonal antibodies. *Am. J. Physiol.* **269**, C1496–C1505.

Mastroianni, N., Bettinelli, A., Bianchetti, M., Colussi, G., De Fusco, M., Sereni, F., Ballabio, A. and Casari, G. (1996). Novel molecular variants of the Na^+–Cl^- cotransporter gene are responsible for Gitelman syndrome. *Am. J. Human Genet.* **59**, 1019–1026.

Matsunaga, H., Yamashita, N., Okuda, T. and Kurokawa, K. (1994). Mesangial cell ion transport and tubuloglomerular feedback. *Curr. Opin. Nephrol. Hypertens.* **3**, 518–522.

Misgeld, U., Deisz, R. A., Dodt, H. U. and Lux, H. D. (1986). The role of chloride transport in postsynaptic inhibition of hippocampal neurons. *Science* **232**, 1413–1415.

Mount, D. B., Hall, A. E., Plata, C., Vilanueva, Y., Kaplan, M. R., Gamba, G. and Hebert, S. C. (1995). Characterization of alternatively spliced transcripts of the murine apical bumetanide-sensitive Na^+–K^+–Cl^- cotransporter gene. *J. Am. Soc. Nephrol.* **6**, 347.

Mount, D. B., Hoover, R. S. and Hebert, S. C. (1997). The molecular physiology of electroneutral cation–chloride cotransport. *J. Membr. Biol.* **158**, 177–186.

Obermüller, N., Bernstein, P., Velazquez, H., Reilly, R., Moser, D., Ellison, D. H. and Bachmann, S. (1995). Expression of the thiazide-sensitive Na^+–Cl^- cotransporter in rat and human kidney. *Am. J. Physiol.* **269**, F900–F910.

Obermüller, N., Kunchaparty, S., Ellison, D. H. and Bachmann, S. (1996). Expression of the Na^+–K^+–$2Cl^-$ cotransporter by macula

densa and thick ascending limb cells of rat and rabbit nephron. *J. clin. Invest.* **98**, 635–640.

PAYNE, J. A. (1997). Functional characterization of the neuronal-specific K^+–Cl^- cotransporter: implications for $[K^+]_o$ regulation. *Am. J. Physiol.* **273**, C1516–C1525.

PAYNE, J. A. AND FORBUSH III, B. (1994). Alternatively spliced isoforms of the putative renal Na^+–K^+–Cl^- cotransporter are differentially distributed within the rabbit kidney. *Proc. natn. Acad. Sci. U.S.A.* **91**, 4544–4548.

PAYNE, J. A., STEVENSON, T. J. AND DONALDSON, L. F. (1996). Molecular characterization of a putative K^+–Cl^- cotransporter in rat brain. A neuronal-specific isoform. *J. biol. Chem.* **271**, 16245–16252.

PAYNE, J. A., XU, J. C., HAAS, M., LYTLE, C. Y., WARD, D. AND FORBUSH III, B. (1995). Primary structure, functional expression and chromosomal localization of the bumetanide-sensitive Na^+–K^+–Cl^- cotransporter in human colon. *J. biol. Chem.* **270**, 17977–17985.

PLOTKIN, M. D., KAPLAN, M. R., VERLANDER, J. W., LEE, W.-S., BROWN, D., POCH, E., GULLANS, S. R. AND HEBERT, S. C. (1996). Localization of the thiazide-sensitive Na^+–Cl^- cotransporter, rTSC1, in the rat kidney. *Kidney Int.* **50**, 174–183.

PLOTKIN, M. D., KAPLAN, M. R., PETERSON, L. N., GULLANS, S. R., HEBERT, S. C. AND DELPIRE, E. (1997*a*). Expression of the Na^+–K^+–$2Cl^-$ cotransporter, BSC2, in the nervous system. *Am. J. Physiol.* **272**, C173–C183.

PLOTKIN, M. D., SNYDER, E. Y., HEBERT, S. C. AND DELPIRE, E. (1997*b*). Expression of the Na–K–2Cl cotransporter is developmentally regulated in postnatal rat brains: a possible mechanism underlying GABA's excitatory role in immature brain. *J. Neurobiol.* **30**, 781–795.

POCH, E., SUASTEGUI, R., GAMBA, G. AND HEBERT, S. C. (1996). Role of N-linked glycosylation in rat thiazide-sensitive Na^+–Cl^- cotransporter. *J. Am. Soc. Nephrol.* **7**, 1288.

POLLAK, M. R., DELANEY, V. B., GRAHAM, R. M. AND HEBERT, S. C. (1996). Gitelman's syndrome (Bartter's variant) maps to the thiazide-sensitive cotransporter gene locus on chromosome 16q13 in a large kindred. *J. Am. Soc. Nephrol.* **7**, 2244–2248.

RAAT, N. J., DELPIRE, E., VAN OS, C. H. AND BINDELS, R. J. (1996). Culturing induced expression of basolateral Na^+–K^+–$2Cl^-$ cotransporter BSC2 in proximal tubule, aortic endothelium and vascular smooth muscle. *Pflügers Arch.* **431**, 458–460.

RANDALL, J., THORNE, T. AND DELPIRE, E. (1997). Partial cloning and characterization of Slc12a2: the gene encoding the secretory Na^+–K^+–$2Cl^-$ cotransporter. *Am. J. Physiol.* **273**, C1267–C1277.

ROCHA, A. S. AND KUDO, L. H. (1990). Atrial peptide and cGMP effects on Na^+–Cl^- transport in inner medullary collecting duct. *Am. J. Physiol.* **259**, F258–F268.

SIMON, D. B., BINDRA, R. S., MANSFIELD, T. A., NELSON-WILLIAMS, C., MENDONCA, E., STONE, R., SCHURMAN, S., NAYIR, A., ALPAY, H., BAKKALOGLU, A., RODRIGUEZ-SORIANO, J., MORALES, J. M., SANJAD, S. A., TAYLOR, C. M., PILZ, D., BREM, A., TRACHTMAN, H., GRISWOLD, W., RICHARD, G. A., JOHN, E. AND LIFTON, R. P. (1997). Mutations in the chloride channel gene, CLCNKB, cause Bartter's syndrome type III. *Nature Genet.* **17**, 171–178.

SIMON, D. B., KARET, F. E., HAMDAN, J. M., DIPIETRO, A., SANJAD, S. A. AND LIFTON, R. P. (1996*a*). Bartter's syndrome, hypokalaemic alkalosis with hypercalciuria, is caused by mutations in the Na–K–2Cl cotransporter NKCC2. *Nature Genet.* **13**, 183–188.

SIMON, D. B., KARET, F. E., RODRIQUEZ-SORIANO, J., HAMDAN, J. H., DIPIETRO, A., TRACHTMAN, H., SANJAD, S. A. AND LIFTON, R. P. (1996*b*). Genetic heterogeneity of Bartter's syndrome revealed by mutations in the K^+ channel, ROMK. *Nature Genet.* **14**, 152–156.

SIMON, D. B., NELSON-WILLIAMS, C., BIA, M. J., ELLISON, D., KARET, F. E., MOLINA, A. M., VAARA, I., IWATA, F., CUSHNER, H. M., KOOLEN, M., GAINZA, F. J., GITLEMAN, H. J. AND LIFTON, R. P. (1996*c*). Gitelman's variant of Bartter's syndrome, inherited hypokalaemic alkalosis, is caused by mutations in the thiazide-sensitive Na–Cl cotransporter. *Nature Genet.* **12**, 24–30.

SOYBEL, D. I., GULLANS, S. R., MAXWELL, F. AND DELPIRE, E. (1995). Role of basolateral Na^+–K^+–Cl^- cotransport in HCl secretion by amphibian gastric mucosa. *Am. J. Physiol.* **269**, C242–C249.

STALEY, K., SMITH, R., SCHAACK, R., WILCOX, C. AND JENTSCH, T. J. (1996). Alteration of $GABA_A$ receptor function following gene transfer of the CLC-2 chloride channel. *Neuron* **17**, 543–551.

STEIN, J. H. (1985). The pathogenetic spectrum of Bartter's syndrome (clinical conference). *Kidney Int.* **28**, 85–93.

STOKES, J. B. (1989). Electroneutral Na^+–Cl^- transport in the distal tubule. *Kidney Int.* **36**, 427–433.

SUN, A., GROSSMAN, E. B., LOMBARDI, M. AND HEBERT, S. C. (1991). Vasopressin alters the mechanism of apical Cl^- entry from Na^+–Cl^- to Na^+–K^+–$2Cl^-$ cotransport in mouse medullary thick ascending limb. *J. Membr. Biol.* **120**, 83–94.

TAKEUCHI, K., KURE, S., KATO, T., TANIYAMA, Y., TAKAHASHI, N., IKEDA, Y., ABE, T., NARISAWA, K., MURAMATSU, Y. AND ABE, K. (1996). Association of a mutation in thiazide-sensitive Na^+–Cl^- cotransporter with familial Gitelman's syndrome. *J. clin. Endocr. Metab.* **81**, 4496–4499.

TANIMURA, A., KURIHARA, K., RESHKIN, S. J. AND TURNER, R. J. (1995). Involvement of direct phosphorylation in the regulation of the rat parotid Na^+–K^+–$2Cl^-$ cotransporter. *J. biol. Chem.* **270**, 25252–25258.

TSUKAHARA, H., KRIVENKO, Y., MOORE, L. C. AND GOLIGORSKY, M. S. (1994). Decrease in ambient $[Cl^-]$ stimulates nitric oxide release from cultured rat mesangial cells. *Am. J. Physiol.* **267**, F190–F195.

TSURUOKA, S., KOSEKI, C., MUTO, S., TABEI, K. AND IMAI, M. (1994). Axial heterogeneity of potassium transport across hamster thick ascending limb of Henle's loop. *Am. J. Physiol.* **267**, F121–F129.

WALL, S. M., TRINH, H. N. AND WOODWARD, K. E. (1995). Heterogeneity of NH_4 transport in mouse inner medullary collecting duct cells. *Am. J. Physiol.* **38**, F536–F544.

XU, J. Z., HALL, A. E., PETERSON, L. N., BIENKOWSKI, M. J., EESSALU, T. E. AND HEBERT, S. C. (1997). Localization of the ROMK protein on apical membranes of rat kidney nephron segments. *Am. J. Physiol.* **273**, F739–F748.

XU, J. C., LYTLE, C., ZHU, T. T., PAYNE, J. A., BENZ, E., JR AND FORBUSH III, B. (1994). Molecular cloning and functional expression of the bumetanide-sensitive Na^+–K^+–Cl^- cotransporter. *Proc. natn. Acad. Sci. U.S.A.* **91**, 2201–2205.

YERBY, T. R., VIBAT, C. R. T., SUN, D., PAYNE, J. A. AND O'DONNELL, M. E. (1997). Molecular characterization of the Na^+–K^+–Cl^- cotransporter of bovine aortic endothelial cells. *Am. J. Physiol.* **273**, C188–C197.

YU, H., PAPA, F. AND SUKHATME, V. P. (1994). Bovine and rodent Tamm–Horsfall protein (THP) genes: cloning, structural analysis and promoter identification. *Gene Expr.* **4**, 63–75.